This is a repository copy of *Key Role of NO3 Radicals in the Production of Isoprene Nitrates and Nitrooxyorganosulfates in Beijing*.

White Rose Research Online URL for this paper:
https://eprints.whiterose.ac.uk/170408/

Version: Accepted Version

Key role of NO$_3$ radicals in the production of isoprene nitrates in Beijing

Jacqueline F. Hamilton[1*], Daniel J. Bryant[1], Pete Edwards[1], Bin Ouyang[2,3], Thomas J. Bannan[4], Archit Mehra[4], James R. Hopkins[1,5], Rachel E. Dunmore[1], Freya A. Squires[1], James D. Lee[1,5], Stephen D. Worrall[4], Asan Bacak[4], Hugh Coe[4], Carl Percival[4,6], Lisa K. Whalley[7], Dwayne E. Heard[7], Eloise J. Slater[7], Tianqu Cui[8], Jason D. Surratt[8], Claire Reeves[9], Graham Mills[9], Sue Grimmond[10], Andrew R. Rickard[1,2]

[1] Wolfson Atmospheric Chemistry Laboratories, Department of Chemistry, University of York, York, UK
[2] Lancaster Environment Centre, Lancaster University, Lancaster, UK
[3] Department of Chemistry, University of Cambridge, Cambridge, UK
[4] School of Earth and Environmental Sciences, The University of Manchester, Manchester, UK
[5] National Centre for Atmospheric Science, University of York, York, UK
[6] now at Jet Propulsion Laboratory, California Institute of Technology, 4800 Oak Grove Drive, Pasadena, CA, USA
[7] School of Chemistry, University of Leeds, Leeds, UK
[8] Department of Environmental Sciences and Engineering, Gillings School of Global and Public Health, University of North Carolina, USA
[9] School of Environmental Studies, University of East Anglia, Norwich, United Kingdom
[10] Department of Meteorology, University of Reading, Reading, United Kingdom

Correspondence to: Jacqueline Hamilton (jacqui.hamilton@york.ac.uk)

Abstract – 200 words max

In urban areas, the formation of isoprene nitrates (IN) can lead to significant secondary organic aerosol (SOA) production and act as reservoirs of atmospheric nitrogen oxides. In this work, we estimate the rate of production of IN from the reactions of isoprene with OH and NO$_3$ radicals during the summertime. While OH dominates the loss rate of isoprene during the day, NO$_3$ can play an important role in the production of IN during both the day and at night. Unusually low NO concentrations during the afternoon resulted in NO$_3$ mixing ratios of around 3 pptv, which we estimated to account for around a third of the total IN production in the gas phase. Heterogenous uptake of IN produces nitroxyorganosulfates (NOS), with two distinct diurnal profiles observed in the particle phase. A mono-nitrated NOS proposed to be the organosulfate (OS) formed from the acid catalyzed uptake of isoprene nitroxy hydroxyepoxide, formed via sequential reaction of isoprene with NO$_3$ and OH radicals, peaked during the day. Di-and tri-nitrated isoprene related NOS, formed

from multiple NO₃ oxidation steps, peaked at night. This work highlights that NO_3 chemistry can play a key role in the formation of IN Beijing during both the day and night.

Introduction

Poor air quality is the biggest environmental factor contributing to premature mortality globally[1]. As the Earth's population has grown, the number of people living in urban areas has increased rapidly from 751 million in 1950 to 4.2 billion in 2018[2]. By 2030, the UN estimates there will be 43 megacities (>10 million inhabitants) with most of them located in developing countries in Africa, Asia and Latin America[2]. Since many of these locations are situated in the tropics, high average temperatures can lead to significant emissions of biogenic volatile organic compounds (VOC) to the urban atmosphere, in particular isoprene of which ~80% globally is emitted from the tropics[3]. Beijing, in China, is a well-studied megacity, with significant air quality issues related to particle pollution and ozone production. Beijing experiences high average summertime temperatures (*ca.* 30 °C) and has a high percentage of green space (> 41 %)[4], which can lead to significant amounts of isoprene being emitted[5]. Photochemical oxidation of isoprene in the presence of high levels of anthropogenic pollutants, in particular nitric oxide (NO) and sulfur dioxide (SO_2), can lead to enhanced secondary organic aerosol production[6–15].

A key uncertainty in understanding SOA production from isoprene is the role of isoprene nitrates (IN). IN are formed in chain terminating reactions, from oxidation by hydroxyl radicals (OH) in the presence of NO, that can reduce ozone production and also act as a sink for atmospheric nitrogen[16]. During the daytime, reaction of isoprene with OH radicals leads to the formation of hydroxy peroxy radicals (ISOPOO), which can react with NO to form isoprene hydroxy nitrates (IHN), with further reactions leading to a suite of multifunctional IN (Wennberg et al., and references therein)[17]. At night, OH levels are much lower and oxidation by NO_3 radicals often becomes a more important loss route for unsaturated hydrocarbon species. Reaction with NO_3 leads to the production of isoprene nitrate peroxy radicals (INO_2), which can then go on to form a range of IN via reactions with HO_2, RO_2 and NO[18,19]. During the daytime VOC +

NO₃ reactions are usually limited by the fast photolysis of NO$_3$ and its reaction with NO.

Recent observations in a boreal forest by Liebmann et al.[20] under low-NO conditions indicated that in some circumstances daytime alkyl nitrate production from NO$_3$ chemistry can dominate over OH. Although Beijing and other megacities may not be obvious low-NO environments, recent observations indicate that in summer NO levels in the afternoon can drop to below 1 ppbv, as a result of reactions with ozone and other unknown chemistry[21]. In this paper, we show the importance of nitrate radical chemistry for the production of IN in the Beijing summer using a comprehensive suite of gas and particle phase observations taken as part of UK-China Air Pollution and Human Health programme.

Site description, sample collection and extraction

Aerosol filter samples were collected between the 18th May and 24th June 2017 at the Institute of Atmospheric Physics (IAP) in Beijing, China[22]. Filter samples were collected at a height of 8 m, on top of a building in the IAP complex every 3 hours between 08:30 and 17:30 and then one overnight sample (17:30-08:30). The samples were collected on preheated (500 ^{o}C for 5 hours) quartz filters (8 by 10 in) using an ECOTECH HiVOL 3000 (Ecotech, Australia) with a selective PM$_{2.5}$ inlet. Samples were collected at a height of 8 m on top of a building at the IAP complex. Filter samples were extracted into high purity water and analysed by UPLC-MS^2, using an Ultimate 3000 UPLC coupled to a Q-Exactive Orbitrap MS, with a heated electrospray ionization using the method in Bryant et al., (2019)[23]. Further details on the method used for calibration can be found in the SI.

A time of flight chemical ionisation mass spectrometer (ToF-CIMS) using an iodide ionisation system was used to measure gas phase isoprene hydroxynitrates in real time[24]. Nitrogen oxide (NO) was measured via chemiluminescence and NO$_2$ via a Cavity Attenuated Phase Shift (CAPS) spectrometer. The meteorological variables of wind speed and direction, relative humidity and temperature were measured at a height of 102 m on the IAP 325 m meteorological tower. VOCs were measured using

a dual channel GC with flame ionisation detectors[25]. The sum of monoterpenes were measured using a proton transfer mass spectrometer (PTR-MS)[26]. Isoprene carbonyl nitrate was measured using negative ionization GC-MS[27]. OH, HO_2 and RO_2 radical measurements were made via two Fluorescence Assay by Gas Expansion (FAGE) detection cells[28,29]. NO_3 and N_2O_5 were measured using a broadband cavity enhanced absorption spectrometer (BBCEAS)[30]. The boundary layer height was measured by a ceilometer[31]. Further information about the site and instrumentation can be found in Shi et al.[22] Campaign average diurnal profiles of isoprene, OH, NO_3 and O_3 can be found in Bryant et al.[23]

Isoprene nitrate production

High ozone mixing ratios (up to 180 ppbv) in Beijing[22] resulted in high NO_3 production rates of the order of 4 ppbv hr^{-1}, peaking in the late afternoon and early evening (Fig. 1c). High daytime NO_3 loss rates, due to rapid photolysis and reaction with NO, resulted in low NO_3 mixing ratios (average = 2-3 pptv, Figure 1c) and it is often assumed that daytime reactions of NO_3 with hydrocarbons are negligible. However, the high levels of biogenic hydrocarbons in Beijing, in particular isoprene, mean that their reaction can compete as an NO_3 loss mechanism. Figure 1a shows the fractional loss of NO_3 calculated from measurements of NO_3 sinks. Although dominated by reaction with NO and photolysis, mean NO_3 loss to isoprene is around 5% in the afternoon across the entire measurement period (Fig. 2b), but reaches as high as 22% prior to sunset on 14th July.
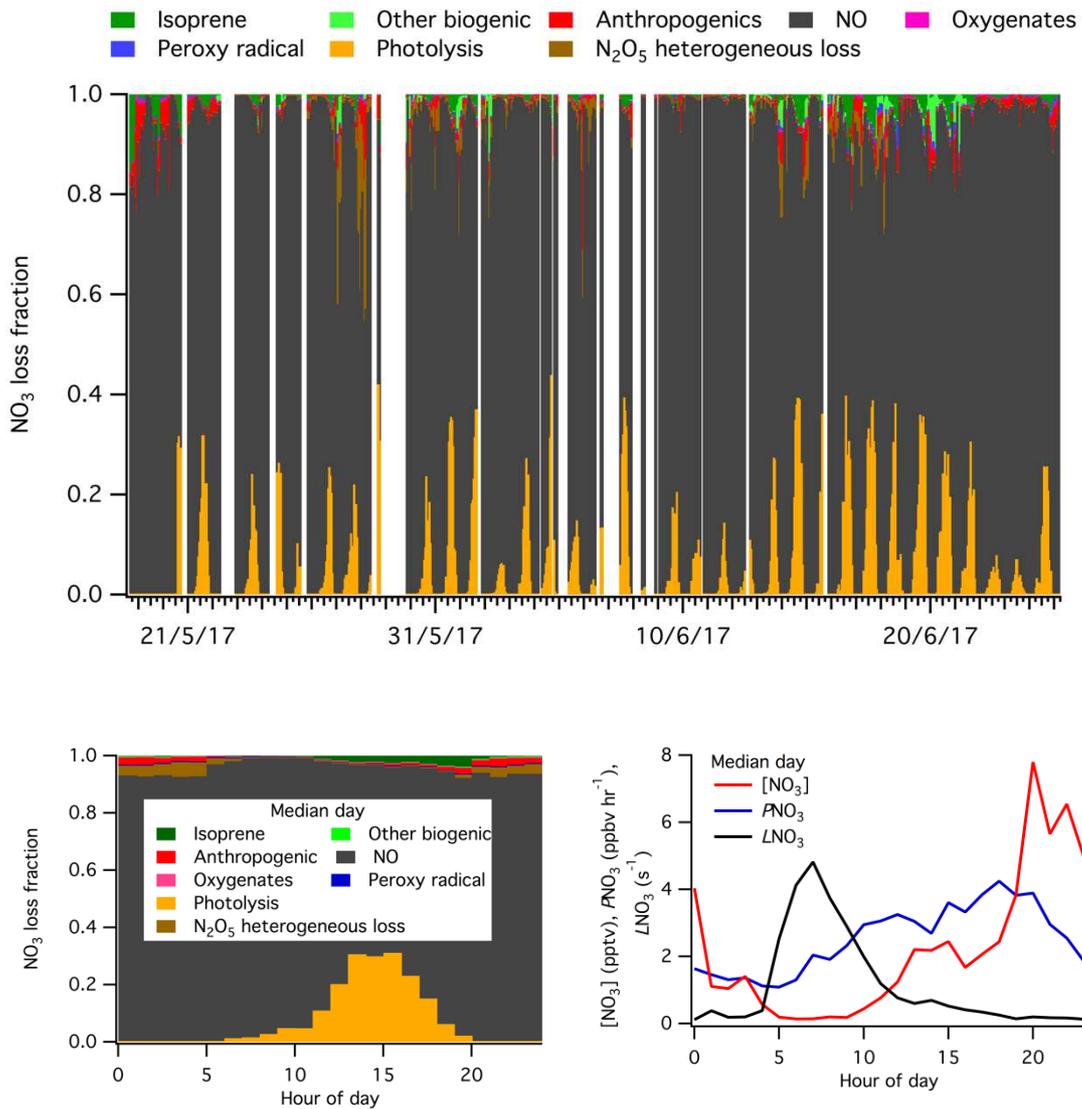
Figure 1a) NO₃ loss fraction calculated using measured NO₃ sinks, including photolysis and heterogeneous losses. An N₂O₅ uptake coefficient of 0.022 has been used based on Tham et al. 2018. b) Daily median of data shown in 1a). c) Daily median NO₃ mixing ratio (pptv), total production (PNO₃) and loss rates (LNO₃) (ppbv hr⁻¹ and s⁻¹ respectively).

Due to high day time emissions of isoprene, its loss rate *via* reaction with NO₃ (L_{NO3} = $k_{NO3}[NO_3][ISO]$) was highest between 13:00 and 18:00, as shown in Figure 2a, with around 65 pptv hr⁻¹ isoprene lost through this route in the afternoon. While this sink of isoprene is minor compared to reaction with OH radicals, the production of isoprene nitrates from NO₃ chemistry becomes important.
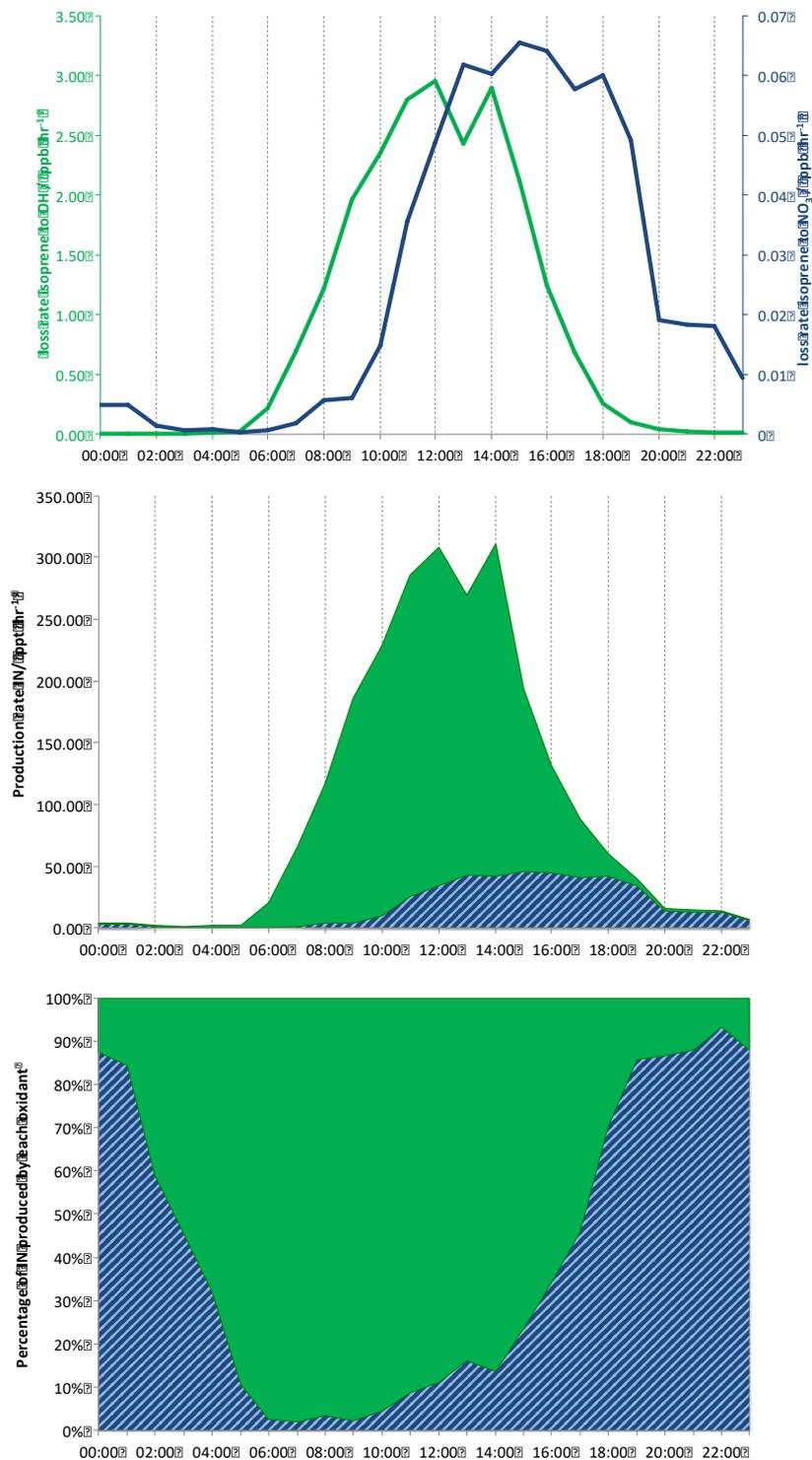
Figure 2: Average diurnal of (a) isoprene loss rate to NO_3 (blue) and OH (green), (b) IN production rate and (c) percentage contribution of each oxidant to IN production.

The production rate of nitrates from isoprene can be estimated using equations 1 and 2, where α is the oxidant specific yield of isoprene nitrates and k_1 and k_2 are the rate constants for the reaction of isoprene with OH and NO_3, respectively.

$$P_{IN\ Iso+OH} = \alpha_1\ k_1\ [OH][Isoprene] \qquad\qquad (1)$$

$$P_{IN\ Iso+NO3} = \alpha_2\ k_2\ [NO_3][Isoprene] \qquad\qquad (2)$$

During the afternoon in Beijing, Newland et al.[21] showed that the fraction of the RO_2, formed from isoprene + OH, reacting with NO can be as low as 65 % (f_{NO} = 0.65), with the remainder reacting with HO_2, RO_2 or undergoing isomerization. Therefore, the production rate of isoprene nitrates from OH chemistry calculated in equation 1 should be multiplied by f_{NO} during the afternoon as shown in equation 3.

$$P_{IN\ Iso+OH} = \alpha_1\ k_1\ [OH][Isoprene] \times f_{NO} \qquad\qquad (3)$$

Using an isoprene nitrate yield (α_1) of 9.2 % from isoprene + OH/NO[32] and (α_2) 70 % yield from isoprene + NO_3 (Schwantes et al. and references within) [18], the calculated isoprene nitrate production rates are shown in Figure 2b. Around midday the total isoprene nitrate production rate ($P_{IN\ total}$ = $P_{IN\ Iso+OH}$ + $P_{IN\ Iso+NO3}$) is 240 pptv hr^{-1}, with approximately 89 % from OH + NO chemistry ($P_{IN\ Iso+OH}$) and 11 % from NO_3 oxidation ($P_{IN\ Iso+NO3}$) as shown in Figure 2c. The CIMS measured the sum of IHN, the first generation nitrates formed from isoprene + OH oxidation, which peaked at midday at around 120 pptv, before dropping off in the late afternoon to a minimum overnight.[23] By 16:00, $P_{IN\ total}$ dropped to ~110 pptv hr^{-1} as a result of the low NO conditions and reduction in isoprene mixing ratios in Beijing, with around 35 % of $P_{IN\ total}$ from NO_3 + isoprene. Measurements of isoprene carbonyl nitrates (ICN) formed from NO_3 chemistry indicate these species peak in the early evening (See SI Figure X). However, even though they are likely to undergo fast photolysis and rapid reaction with OH[33] they are present during the daytime at low concentrations indicating considerable daytime production from isoprene + NO_3 chemistry.

Therefore, even though only a small fraction of isoprene reacts with NO_3 during the afternoon (2 %, shown in Figure 1a), it can represent a significant source of isoprene nitrate.

Particulate isoprene nitroxyorganosulfates (NOS)

The UPLC-ESI-MS methodology used to study the composition of Beijing organic aerosol[23] was not suited to analyzing nitrates. However, it does give a strong signal for the sulfated versions of the nitrates, NOS. Nine isoprene-derived NOS compounds were observed in the Beijing samples and their mean, median and maximum observed concentrations are shown in Table 1. Two isoprene derived mono-nitrated tracers were observed that followed similar temporal trends as other isoprene OS, peaking generally during the afternoon, and with a strong correlation with particulate sulfate. Four isoprene derived di-nitrated NOS and three tri-nitrated NOS were also observed, all showing a strong enhancement during the night.

Mono-nitrate NOS

A NOS ($C_5H_{11}NSO_9$) consistent with 2-methyltetrol nitrate OS, was observed and the time series is shown in Figure 3a. This species had a mean concentration of 12.6 ng m^{-3} and a maximum of 154 ng m^{-3}. This mean concentration is similar to that of 2-methyltetrol-OS (2-MT-OS), observed during the same period (mean = 11.8 ng m^{-3}). This species generally peaked during the samples taken during the late afternoon, as shown in figure 4a, although there is not a very strong diurnal profile. Wang et al.[34] also observed a daytime peak for this species at Changping, a site 38 km north east of Beijing. This NOS species was observed to have a reasonably strong correlation with particulate sulfate ($R^2 = 0.61$) and a strong correlation with the product of the concentration of gas phase ozone and particle phase sulfate [O_3][SO_4] ($R^2 = 0.79$). This NOS species also correlated well with the other isoprene derived OS formed from isoprene oxidation by OH observed in Bryant et al.[23] (2-MT-OS, $R^2 = 0.51$; 2-methylglyceric acid-OS, $R^2 = 0.58$; $C_5H_{10}SO_6$, $R^2 = 0.82$). We propose that this NOS compound is formed from the acid catalysed heterogeneous uptake of an isoprene nitroxy hydroxyepoxide (INHE)[18], as shown in Scheme 1.
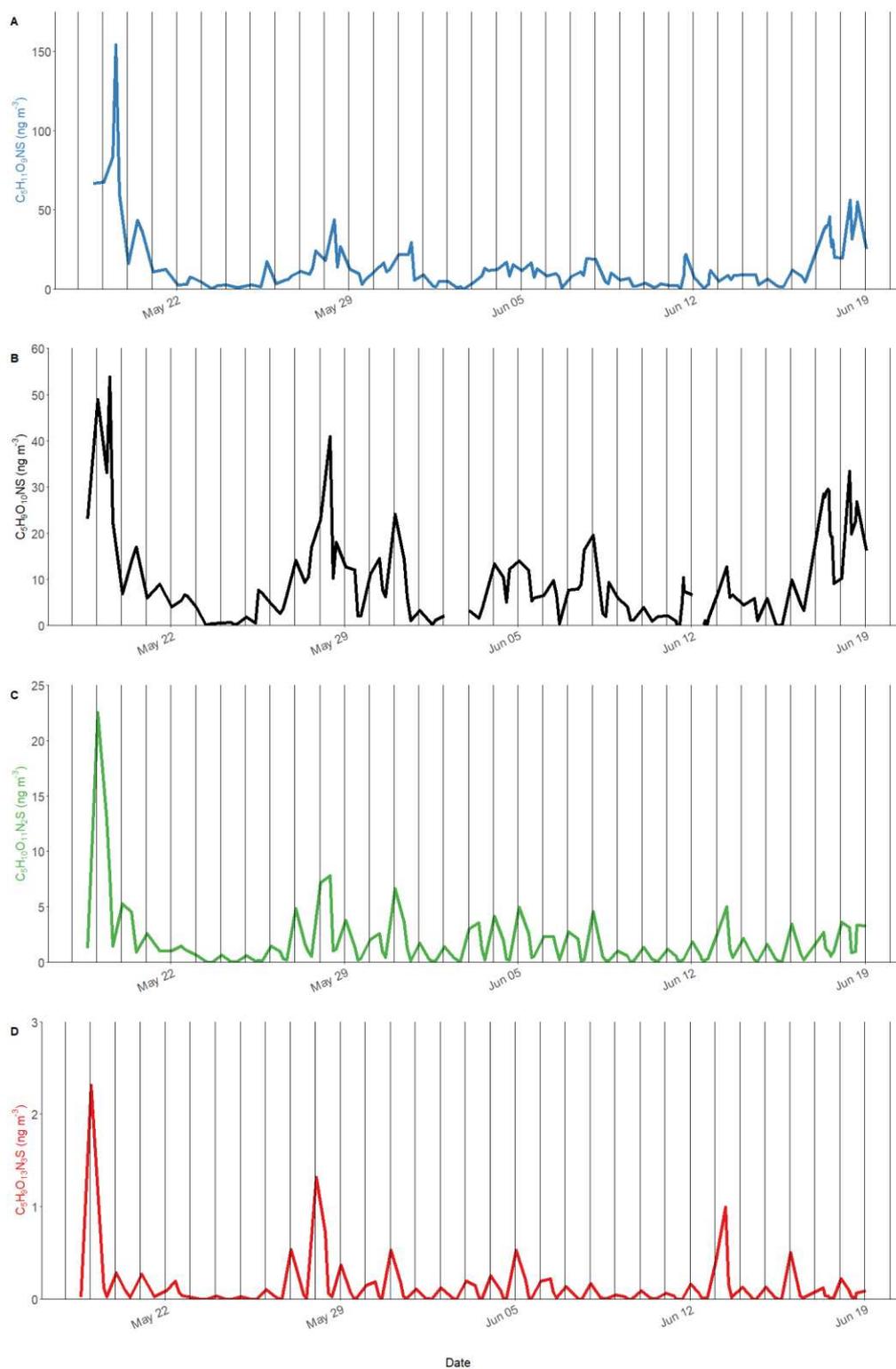
Figure 3. Time series the measured concentrations of NOS in Beijing aerosol. The vertical lines are at midnight of each day of sampling. A) $C_5H_{11}O_9NS$, B) $C_5H_9O_{10}NS$, C) Sum of $C_5H_{10}O_{11}N_2S$ species, D) Sum of $C_5H_9O_{13}N_3S$ species.

The reaction of isoprene with NO_3 radicals leads to isoprene nitrate peroxy radicals (INO_2). Under atmospherically relevant RO_2 lifetimes, INO_2 can react with HO_2, leading to the formation of isoprene nitroxy hydroperoxide (INP) as shown in the upper part

of Scheme 1. There are 6 INP isomers possible and only the most abundant isomer (δ-[1,4]-INP) observed by Schwantes et al.[18] is shown in the scheme. Reaction of INP with OH radicals, followed by OH recycling, can lead to INHE (two possible isomers, β-[4,1]-INHE and β-[2,1]-INHE) in a similar way to the formation of isoprene derived dihydroxyepoxides (IEPOX) from the reaction of OH with isoprene hydroxy hydroperoxides (ISOPOOH)[35]. Schwantes et al.[18] also showed that INHE could undergo reactive uptake to highly acidified aerosol similar to IEPOX.

INP, the precursor to INHE, only forms from NO_3 oxidation of isoprene. In Schwantes et al.[18] it was proposed that any INP formed overnight and still remaining at sunrise could undergo OH oxidation to form INHE. Our ambient observations indicate that the low NO concentrations in Beijing during the afternoon could enhance the production of daytime INHE in this polluted environment due to two factors. First, the loss rate of NO_3 via reactions with NO is reduced leading to a longer NO_3 daytime lifetime, as indicated by the sustained observed levels of afternoon NO_3. Secondly, the INO_2 radicals that form from NO_3 + isoprene chemistry will have a longer lifetime under low NO conditions and thus a higher fraction will react with HO_2 to form INP. INP produced in the daytime can then readily react with OH to form INHE.

Scheme 1: Proposed formation pathways of mono-nitrated OS and di-nitrated OS species observed in the aerosol from the NO_3 initiated oxidation of isoprene. Note only one of six possible INP isomers is shown for simplicity, with the δ-[1,4]-INP and β-[1,2]-INP the dominant isomers observed in Schwantes et al.[36]

2-methyltetrol nitrate OS
$C_5H_{10}NO_9S^-$
MW = 260.20

H⁺, SO₄²⁻ aerosol

-[2,1]-INHE: $C_5H_9NO_5$

-OH

-[1,4]-INP: $C_5H_9NO_5$

Isoprene

NO₃/O₂

-[1,4]-INO₂

HO₂

·OH

NO₃

dihydroxy-dinitrate OS
$C_5H_9N_2O_{11}S^-$
MW 305.20

H⁺, SO₄²⁻ aerosol

isoprene dinitrate epoxide
$C_5H_8N_2O_7$

-OH
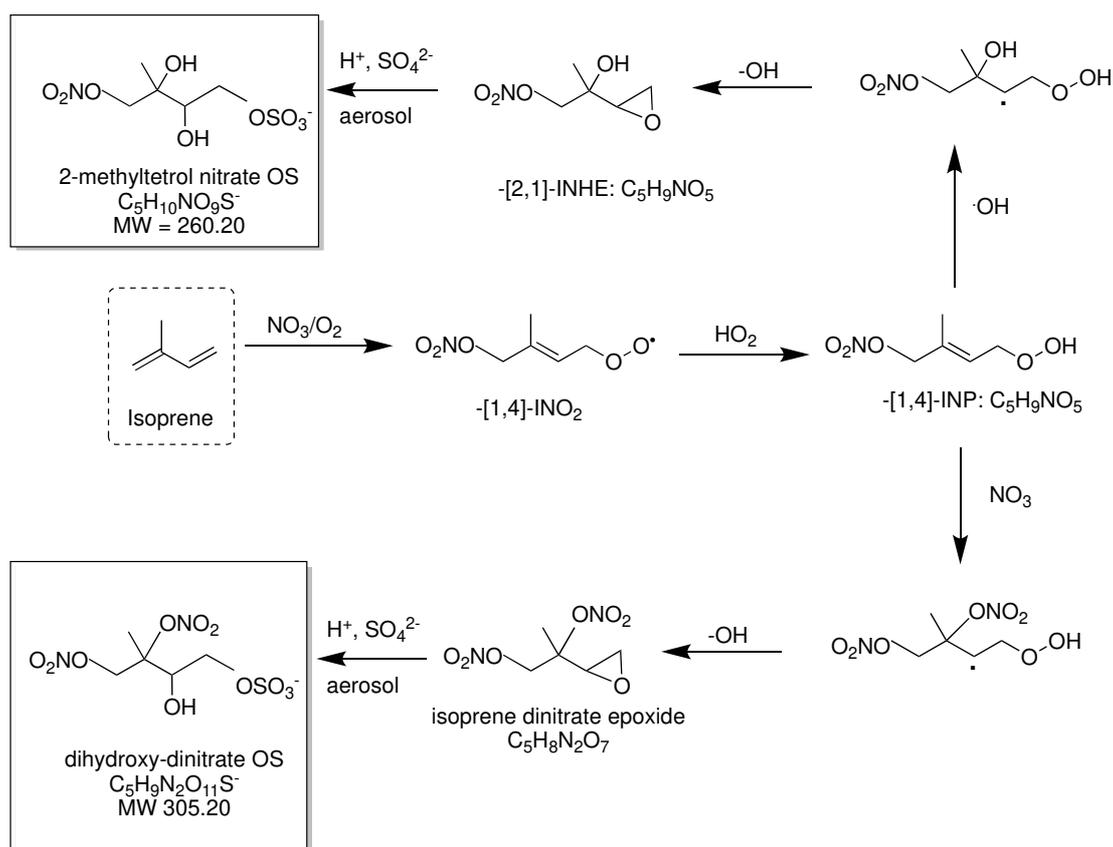
A second isoprene-derived mono-NOS ($C_5H_9NSO_{10}$) was observed and the time series is shown in figure 3b. This species had a mean concentration during the campaign of 9 ng m⁻³ and a maximum of 53.8 ng m⁻³. Of all the isoprene SOA tracers observed previously[23], this compound correlated mostly strongly with the 2-methyltetrol NOS ($R^2 = 0.79$). Nestorowicz et al.[37] identified this species as a highly oxidized NOS tracer formed from 2-methylthreonic acid in isoprene SOA collected during photo-oxidation experiments in the presence of NO. Here, we suggest that this isoprene NOS species comes from the oxidation of the isoprene nitroxy aldehyde (a C_5 carbonyl nitrate species (ICN))[18,32,38] subsequently formed from the reaction of a nitrate peroxy radical (INO₂) with NO, NO₃ and/or another RO₂ species, or from the reaction of isoprene nitroxy hydroperoxide (INP) with OH (in an alternative reaction pathway to the formation of INHE (Scheme 1)). This ICN species can react with NO₃ or OH, leading to the formation of the observed NOS species as shown in Figure SX in the supplementary material.

Di- and tri-nitrated NOS

Four of the isoprene-derived NOS species are di-nitrates ($C_5H_{10}O_{11}N_2S$, retention times 1.56, 1.86, 2.18 and 3.6 mins) and three are tri-nitrates ($C_5H_9O_{13}N_3S$, retention times 5.34, 5.49, 5.90 mins). The time series of the sum of the di- and tri-nitrated NOS are shown in Figure 3c and 3d respectively. The sum of the four isoprene dinitrate isomers ($C_5H_{10}O_{11}N_2S$) had an average concentration of 2.6 ng m^{-3} and a maximum of 23 ng m^{-3}. The trinitrate-OS ($C_5H_9O_{13}N_3S$) were observed at much lower concentrations, with an average of 0.2 ng m^{-3} and a maximum of 2.3 ng m^{-3}. These isoprene-derived NOS had moderate to strong correlations with each other as shown in SI figure 1 (R^2 = 0.76-0.99).

Figure 4c shows box whisker plots of the di-nitrated NOS concentrations split by the sampling time (night, morning, midday and afternoon). These NOS species show a strong enhancement at night, with the mean concentration observed (3.43 ng m^{-3}) around 7.3 times higher than during the afternoon (0.47 ng m^{-3}). These NOS tracers have all previously been observed in chamber studies of NO_3 oxidation of isoprene[19,39,40]. Di-hydroxy di-nitrates have also been observed during the oxidation of isoprene by OH in the presence of NO[40], but this is assumed to be a minor NOS formation route in Beijing due to their enhancement in night time samples.
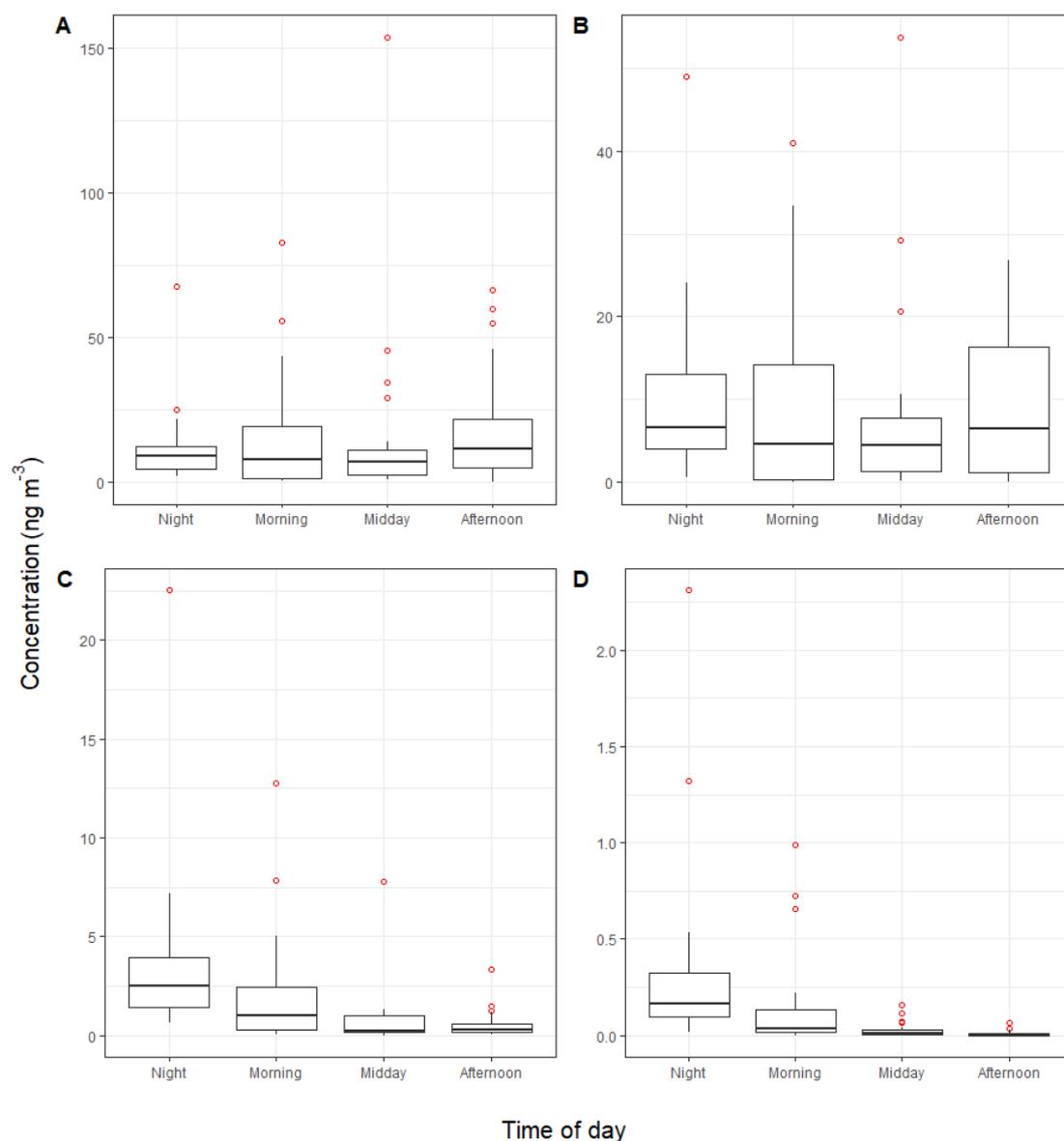
Figure 4. Box and whisker plots of observed NOS concentrations separated by the time of day the filter was collected. A) $C_5H_{11}O_9NS$, B) $C_5H_9O_{10}NS$, C) $C_5H_{10}O_{11}N_2S$, D) $C_5H_9O_{13}N_3S$.

Ng et al.[19] proposed the formation of di- and tri-nitrated OS *via* the formation an isoprene hydroxynitrate (IHN) from INO_2 + INO_2 self-reactions after the initial NO_3 attack. A second NO_3 oxidation step at the other double bond then leads to formation of dihydroxy-dinitrates, again via reaction with INO_2 radicals. A subsequent unknown reaction step with particulate sulfate is then postulated to lead to NOS formation. Here we propose an alternative method where this species is formed via heterogenous uptake of a di-nitrated epoxide as shown in the lower section of Scheme 1. Similar to the mono-nitrate formation, NO_3 reaction with isoprene leads to INO_2

and reaction with HO_2 leads to the isoprene nitrate peroxide (INP). Subsequent addition of a second NO_3 to the C_2 position of the remaining double bond leads to an alkyl radical on the C_3 position. This radical then undergoes a unimolecular decomposition, leading to the formation of an OH radical and a di-nitrated epoxide as proposed in Kwan et al.[41]. Again, this mechanism is very similar to the production of IEPOX from ISOPOOH[35], except in this case rather than being OH neutral (as in the mono-nitrate route to INHE in Scheme1), it can act as a net source of OH radicals at night. Using an OH yield of 0.15, based on Wennberg et al.[42], the calculated OH production rate from this pathway between 19:00 and 22:00 was relatively small, of the order of 2-5 x 10^4 molecules cm^{-3} s^{-1}. The resulting di-nitrated epoxide (IDNE) can then undergo heterogenous uptake to acidic aerosols to form either di-hydroxy-di-nitrates *via* reaction with water or di-nitrated hydroxy OS from reaction with sulfate.

The isoprene-derived di- and tri-nitrated OSs exhibited a strong diurnal profile as shown in figure 4c and 4d, peaking in the night time samples, suggesting their formation is a result of multiple steps of NO_3 oxidation. This is in contrast to the INHE derived mono-nitrate outlined above that formed as a result of NO_3 oxidation followed by OH oxidation. The correlation of the di- and tri-nitrated NOS with particle sulfate is much weaker than the mono-nitrated NOS as shown in Figure S1. The highest levels of the night-time di- and tri- nitrated OSs were observed in samples collected during periods when the highest levels of NO_3 radicals were measured (26/05/2017 NO_3 = 63 ppt, 27/05/17 NO_3 = 69 ppt, see Figure S2). There is not a direct correlation with the average night-time NO_3 mixing ratio (R^2=0.1) but there is a weak correlation with the maximum production rate of NO_3 (P_{NO3}, R^2=0.29) calculated during each filter sampling period. Production of these NOS species is predicted to be highest just after sunset (ca. 19:15-19:30), when residual isoprene can react with increased levels of NO_3, resulting from lower levels of photolysis. The production will then reduce rapidly as the isoprene and NO_3 are consumed, with NO_3 dropping to around 1 pptv by 00:00-03:00 on most nights (See Figure S2). The strong enhancement of these di- and tri-nitrated NOS at night, in comparison to the INHE related mono-nitrate, may indicate that their common precursor INP reacts with OH radicals during the day, and the

products that require two NO_3 oxidation steps therefore only form when OH levels drop at sunset. The formation route of the tri-nitrated species remains uncertain.

The diurnal profile of the di-nitrate and tri-nitrated NOS shows a surprisingly rapid drop in concentration during the daytime. In a previous study of highly oxidised organic nitrates using CIMS, the optimum model-observation agreement was achieved using a short atmospheric lifetime of the order of 2-4 hours[14,43]. Therefore, the diurnal profile seen in Beijing is likely the result of rapid in-particle loss of di- and tri-nitrate OS, such as hydrolysis or oxidation.[44] This may lead to particle phase inorganic nitrate formation and act as a relatively small sink of atmospheric NO_x in Beijing.

On most days there was also an appreciable amount of these NOS species in the samples collected between 08:30 and 11:30, as shown in figure 4b, followed by a rapid decline with a minimum during the late afternoon sample. We suggest that the relatively high abundance of these species during the early morning sample may be the result of mixing down of regionally produced NOS from the nocturnal residual layer during the collapse of the nocturnal boundary layer (Figure S3).

The average diurnal profile of the observed mixing layer height during the campaign, shows a shallow nocturnal boundary layer with a minimum around 250 m at midnight, then increasing from around 08:00 to a maximum of around 1000 m at 15:00 (Figure S3). The ratio of 1,2,3-butanetricarboxylic acid (MBTCA) to pinonic acid has been suggested in previous studies as an indicator of aerosol age[45,46]. The MBTCA:pinonic acid ratio is shown in Figure S4 and generally peaks in the 08:30-11:30 sample on most days. Therefore the abundance of isoprene-derived di- and tri-nitrate OS in Beijing in summertime is driven by both local nighttime NO_3 chemistry, most likely in the early evening when the nitrate radical concentrations are increasing (and OH decreasing) as the sun goes down and isoprene is still present in reasonable amounts, and mixing down of aged aerosol in the morning from more regional sources as the nocturnal boundary layer collapses. Unfortunately, the long nocturnal filter sampling time (15 hours) in this study does not allow the full dynamics of the night formation of NOS to

be observed and increased temporal resolution is needed to determine the relative role of isoprene, NO_3 and sulfate aerosol.

Our observations show that the reaction of isoprene with NO_3 leads to the formation of isoprene derived nitrates (IN) in both the gas and particle phases in Beijing in the summer, and that the nitrate radical plays a key role in the formation of IN both during the day and at night.

Table 1. Molecular formulae, negative ion masses, retention times (RT), time weighted means (ng m^{-3}), maximum and minimum concentrations and original source of tracer. BD= Below detection

Isoprene Tracer	[M-H]$^{-1}$	RT (min)	Time weighted mean (ng m^{-3})	Maximum (ng m^{-3})	Minimum (ng m^{-3})	Reference
$C_5H_{11}O_9NS$	260.0082	0.86	12.6	154.1	0.10	Surratt et al., 2008 [39]
$C_5H_9O_{10}NS$	273.9874	0.94	9.17	53.8	BD	Nestorowicz et al., 2018 [37]
$C_5H_{10}O_{11}N_2S$	304.9783	2.18	1.04	8.62	BD	Surratt et al., 2008 [39]
$C_5H_{10}O_{11}N_2S$	304.9783	1.89	0.83	7.69	BD	Surratt et al., 2008 [39]
$C_5H_{10}O_{11}N_2S$	304.9783	1.56	0.42	2.90	BD	Surratt et al., 2008 [39]
$C_5H_{10}O_{11}N_2S$	304.9783	3.60	0.31	3.32	BD	Surratt et al., 2008 [39]
$C_5H_9O_{13}N_3S$	349.9783	5.90	0.19	2.04	BD	Ng et al., 2008 [19]
$C_5H_9O_{13}N_3S$	349.9783	5.49	0.02	0.17	BD	Ng et al., 2008 [19]
$C_5H_9O_{13}N_3S$	349.9783	5.34	0.008	0.10	BD	Ng et al., 2008 [19]

References

(1)   WHO. World Health Organization Releases 7 Million Premature Deaths Annually Linked to Air Pollution. *Accessed June 21.2018. http//www.who.int/mediacentre/news/releases/2014/air-pollution/en/* **2014**, *66*, 37–39.

(2)   Nations, U.; of Economic, D.; Affairs, S.; Division, P. *World Urbanization Prospects The 2018 Revision*; 2018.

(3)   Guenther, A.; Karl, T.; Harley, P.; Wiedinmyer, C.; Palmer, P. I.; Geron, C. Estimates of Global Terrestrial Isoprene Emissions Using MEGAN (Model of Emissions of Gases and Aerosols from Nature). *Atmos. Chem. Phys.* **2006**, *6* (11), 3181–3210. https://doi.org/10.5194/acp-6-3181-2006.

(4)   Huang, C.; Yang, J.; Lu, H.; Huang, H.; Yu, L. Green Spaces as an Indicator of Urban Health: Evaluating Its Changes in 28 Mega-Cities. *Remote Sens.* **2017**, *9* (12), 1266. https://doi.org/10.3390/rs9121266.

(5)   Mo, Z.; Shao, M.; Wang, W.; Liu, Y.; Wang, M.; Lu, S. Evaluation of Biogenic Isoprene Emissions and Their Contribution to Ozone Formation by Ground-Based Measurements in Beijing, China. *Sci. Total Environ.* **2018**, *627*, 1485–1494. https://doi.org/10.1016/J.SCITOTENV.2018.01.336.

(6)   Shrivastava, M.; Andreae, M. O.; Artaxo, P.; Barbosa, H. M. J.; Berg, L. K.; Brito, J.; Ching, J.; Easter, R. C.; Fan, J.; Fast, J. D.; et al. Urban Pollution Greatly Enhances Formation of Natural Aerosols over the Amazon Rainforest. *Nat. Commun.* **2019**, *10* (1), 1046. https://doi.org/10.1038/s41467-019-08909-4.

(7)   Glasius, M.; Bering, M. S.; Yee, L. D.; de Sá, S. S.; Isaacman-VanWertz, G.;

Wernis, R. A.; Barbosa, H. M. J.; Alexander, M. L.; Palm, B. B.; Hu, W.; et al. Organosulfates in Aerosols Downwind of an Urban Region in Central Amazon. *Environ. Sci. Process. Impacts* **2018**, *20* (11), 1546–1558. https://doi.org/10.1039/C8EM00413G.

(8)   Hettiyadura, A. P. S.; Al-Naiema, I. M.; Hughes, D. D.; Fang, T.; Stone, E. A. Organosulfates in Atlanta, Georgia: Anthropogenic Influences on Biogenic Secondary Organic Aerosol Formation. *Atmos. Chem. Phys.* **2019**, *19* (5), 3191–3206. https://doi.org/10.5194/acp-19-3191-2019.

(9)   Chan, M. N.; Surratt, J. D.; Chan, A. W. H.; Schilling, K.; Offenberg, J. H.; Lewandowski, M.; Edney, E. O.; Kleindienst, T. E.; Jaoui, M.; Edgerton, E. S.; et al. Influence of Aerosol Acidity on the Chemical Composition of Secondary Organic Aerosol from Β-Caryophyllene. *Atmos. Chem. Phys.* **2011**, *11* (4), 1735–1751. https://doi.org/10.5194/acp-11-1735-2011.

(10)   Riva, M.; Da Silva Barbosa, T.; Lin, Y.-H.; Stone, E. A.; Gold, A.; Surratt, J. D. Chemical Characterization of Organosulfates in Secondary Organic Aerosol Derived from the Photooxidation of Alkanes. *Atmos. Chem. Phys.* **2016**, *16* (17), 11001–11018. https://doi.org/10.5194/acp-16-11001-2016.

(11)   Surratt, J. D.; Kroll, J. H.; Kleindienst, T. E.; Edney, E. O.; Claeys, M.; Sorooshian, A.; Ng, N. L.; Offenberg, J. H.; Lewandowski, M.; Jaoui, M.; et al. Evidence for Organosulfates in Secondary Organic Aerosol. *Environ. Sci. Technol.* **2007**, *41* (2), 517–527. https://doi.org/10.1021/es062081q.

(12)   Gómez-González, Y.; Surratt, J. D.; Cuyckens, F.; Szmigielski, R.; Vermeylen, R.; Jaoui, M.; Lewandowski, M.; Offenberg, J. H.; Kleindienst, T. E.; Edney, E. O.; et al. Characterization of Organosulfates from the Photooxidation of Isoprene and Unsaturated Fatty Acids in Ambient Aerosol Using Liquid Chromatography/(−) Electrospray Ionization Mass Spectrometry. *J. Mass Spectrom.* **2008**, *43* (3), 371–382. https://doi.org/10.1002/jms.1329.

(13)   Rattanavaraha, W.; Chu, K.; Budisulistiorini, S. H.; Riva, M.; Lin, Y.-H.; Edgerton, E. S.; Baumann, K.; Shaw, S. L.; Guo, H.; King, L.; et al. Assessing the Impact of Anthropogenic Pollution on Isoprene-Derived Secondary Organic Aerosol Formation in PM≪Sub≫2.5≪/Sub≫ Collected from the Birmingham, Alabama, Ground Site during the 2013 Southern Oxidant and Aerosol Study. *Atmos. Chem. Phys.* **2016**, *16* (8), 4897–4914. https://doi.org/10.5194/acp-16-4897-2016.

(14)   Lee, B. H.; Mohr, C.; Lopez-Hilfiker, F. D.; Lutz, A.; Hallquist, M.; Lee, L.; Romer, P.; Cohen, R. C.; Iyer, S.; Kurtén, T.; et al. Highly Functionalized Organic Nitrates in the Southeast United States: Contribution to Secondary Organic Aerosol and Reactive Nitrogen Budgets. *Proc. Natl. Acad. Sci. U. S. A.* **2016**, *113* (6), 1516–1521. https://doi.org/10.1073/pnas.1508108113.

(15)   Hu, J.; Wang, P.; Ying, Q.; Zhang, H.; Chen, J.; Ge, X.; Li, X.; Jiang, J.; Wang, S.; Zhang, J.; et al. Modeling Biogenic and Anthropogenic Secondary Organic Aerosol in China. *Atmos. Chem. Phys.* **2017**, *17* (1), 77–92. https://doi.org/10.5194/acp-17-77-2017.

(16)   Ng, N. L.; Brown, S. S.; Archibald, A. T.; Atlas, E.; Cohen, R. C.; Crowley, J. N.; Day, D. A.; Donahue, N. M.; Fry, J. L.; Fuchs, H.; et al. Nitrate Radicals and Biogenic Volatile Organic Compounds: Oxidation, Mechanisms, and Organic Aerosol. *Atmos. Chem. Phys.* **2017**, *17* (3), 2103–2162.

https://doi.org/10.5194/acp-17-2103-2017.

(17)   Wennberg, P. O.; Bates, K. H.; Crounse, J. D.; Dodson, L. G.; McVay, R. C.; Mertens, L. A.; Nguyen, T. B.; Praske, E.; Schwantes, R. H.; Smarte, M. D.; et al. Gas-Phase Reactions of Isoprene and Its Major Oxidation Products. *Chem. Rev.* **2018**, *118* (7), 3337–3390. https://doi.org/10.1021/acs.chemrev.7b00439.

(18)   Schwantes, R. H.; Teng, A. P.; Nguyen, T. B.; Coggon, M. M.; Crounse, J. D.; St. Clair, J. M.; Zhang, X.; Schilling, K. A.; Seinfeld, J. H.; Wennberg, P. O. Isoprene NO $_3$ Oxidation Products from the RO $_2$ + HO $_2$ Pathway. *J. Phys. Chem. A* **2015**, *119* (40), 10158–10171. https://doi.org/10.1021/acs.jpca.5b06355.

(19)   Ng, N. L.; Kwan, A. J.; Surratt, J. D.; Chan, A. W. H.; Chhabra, P. S.; Sorooshian, A.; Pye, H. O. T.; Crounse, J. D.; Wennberg, P. O.; Flagan, R. C.; et al. Secondary Organic Aerosol (SOA) Formation from Reaction of Isoprene with Nitrate Radicals (NO<Sub>3</Sub>). *Atmos. Chem. Phys.* **2008**, *8* (14), 4117–4140. https://doi.org/10.5194/acp-8-4117-2008.

(20)   Liebmann, J.; Sobanski, N.; Schuladen, J.; Karu, E.; Hellen, H.; Hakola, H.; Zha, Q.; Ehn, M.; Riva, M.; Heikkinen, L.; et al. Alkyl Nitrates in the Boreal Forest: Formation via the NO3-, OH- and O-3-Induced Oxidation of Biogenic Volatile Organic Compounds and Ambient Lifetimes. *Atmos. Chem. Phys.* **2019**, *19* (15), 10391–10403. https://doi.org/10.5194/acp-19-10391-2019.

(21)   Newland, M.; Bryant, D. J.; Dunmore, R. E.; Bannan, T. J.; Acton, W. J.; Langford, B.; Hopkins, J. R.; Squires, F.; Dixon, W.; Drysdale, W.; et al. Rainforest-like Atmospheric Chemistry in a Polluted Megacity. *Press* **2019**.

(22)   Shi, Z.; Vu, T.; Kotthaus, S.; Harrison, R. M.; Grimmond, S.; Yue, S.; Zhu, T.; Lee, J.; Han, Y.; Demuzere, M.; et al. Introduction to the Special Issue "In-Depth Study of Air Pollution Sources and Processes within Beijing and Its Surrounding Region (APHH-Beijing)." *Atmos. Chem. Phys.* **2019**, *19* (11), 7519–7546. https://doi.org/10.5194/acp-19-7519-2019.

(23)   Bryant, D. J.; Dixon, W.; Hopkins, J. R.; Dunmore, R. E.; Pereira, K.; Shaw, M.; Squires, F.; Bannan, T. J.; Mehra, A.; Worrall, S. D.; et al. Strong Anthropogenic Control of Secondary Organic Aerosol Formation from Isoprene in Beijing. *Press* **2019**.

(24)   Le Breton, M.; Wang, Y.; Hallquist, Å. M.; Pathak, R. K.; Zheng, J.; Yang, Y.; Shang, D.; Glasius, M.; Bannan, T. J.; Liu, Q.; et al. Online Gas- and Particle-Phase Measurements of Organosulfates, Organosulfonates and Nitrooxy Organosulfates in Beijing Utilizing a FIGAERO ToF-CIMS. *Atmos. Chem. Phys.* **2018**, *18* (14), 10355–10371. https://doi.org/10.5194/acp-18-10355-2018.

(25)   Hopkins, J. R.; Jones, C. E.; Lewis, A. C. A Dual Channel Gas Chromatograph for Atmospheric Analysis of Volatile Organic Compounds Including Oxygenated and Monoterpene Compounds. *J. Environ. Monit.* **2011**, *13* (8), 2268. https://doi.org/10.1039/c1em10050e.

(26)   Huang, Z.; Zhang, Y.; Yan, Q.; Zhang, Z.; Wang, X. Real-Time Monitoring of Respiratory Absorption Factors of Volatile Organic Compounds in Ambient Air by Proton Transfer Reaction Time-of-Flight Mass Spectrometry. *J. Hazard. Mater.* **2016**, *320*, 547–555. https://doi.org/10.1016/J.JHAZMAT.2016.08.064.

(27) Fu, P.; Kawamura, K.; Kanaya, Y.; Wang, Z. Contributions of Biogenic Volatile Organic Compounds to the Formation of Secondary Organic Aerosols over Mt. Tai, Central East China. *Atmos. Environ.* **2010**, *44* (38), 4817–4826. https://doi.org/10.1016/j.atmosenv.2010.08.040.

(28) Whalley, L. K.; Stone, D.; Dunmore, R.; Hamilton, J.; Hopkins, J. R.; Lee, J. D.; Lewis, A. C.; Williams, P.; Kleffmann, J.; Laufs, S.; et al. Understanding in Situ Ozone Production in the Summertime through Radical Observations and Modelling Studies during the Clean Air for London Project (ClearfLo). *Atmos. Chem. Phys.* **2018**, *18* (4), 2547–2571. https://doi.org/10.5194/acp-18-2547-2018.

(29) Whalley, L. K.; Furneaux, K. L.; Goddard, A.; Lee, J. D.; Mahajan, A.; Oetjen, H.; Read, K. A.; Kaaden, N.; Carpenter, L. J.; Lewis, A. C.; et al. The Chemistry of OH and HO2 Radicals in the Boundary Layer over the Tropical Atlantic Ocean. *Atmos. Chem. Phys.* **2010**, *10* (4), 1555–1576. https://doi.org/10.5194/acp-10-1555-2010.

(30) Zhou, W.; Zhao, J.; Ouyang, B.; Mehra, A.; Xu, W.; Wang, Y.; Bannan, T. J.; Worrall, S. D.; Priestley, M.; Bacak, A.; et al. Production of N&Lt;Sub&Gt;2&Lt;/Sub&Gt;O&Lt;Sub&Gt;5 &Lt;/Sub&Gt; and ClNO&Lt;Sub&Gt;2&Lt;/Sub&Gt; in Summer in Urban Beijing, China. *Atmos. Chem. Phys.* **2018**, *18* (16), 11581–11597. https://doi.org/10.5194/acp-18-11581-2018.

(31) Kotthaus, S.; Grimmond, C. S. B. Atmospheric Boundary-Layer Characteristics from Ceilometer Measurements. Part 1: A New Method to Track Mixed Layer Height and Classify Clouds. *Q. J. R. Meteorol. Soc.* **2018**, *144* (714), 1525–1538. https://doi.org/10.1002/qj.3299.

(32) Jenkin, M. E.; Young, J. C.; Rickard, A. R. The MCM v3.3.1 Degradation Scheme for Isoprene. *Atmos. Chem. Phys.* **2015**, *15* (20), 11433–11459. https://doi.org/10.5194/acp-15-11433-2015.

(33) Xiong, F.; Borca, C. H.; Slipchenko, L. V.; Shepson, P. B. Photochemical Degradation of Isoprene-Derived 4,1-Nitrooxy Enal. *Atmos. Chem. Phys.* **2016**, *16* (9), 5595–5610. https://doi.org/10.5194/acp-16-5595-2016.

(34) Wang, Y.; Hu, M.; Guo, S.; Wang, Y.; Zheng, J.; Yang, Y.; Zhu, W.; Tang, R.; Li, X.; Liu, Y.; et al. The Secondary Formation of Organosulfates under Interactions between Biogenic Emissions and Anthropogenic Pollutants in Summer in Beijing. *Atmos. Chem. Phys.* **2018**, *18* (14), 10693–10713. https://doi.org/10.5194/acp-18-10693-2018.

(35) Paulot, F.; Crounse, J. D.; Kjaergaard, H. G.; Kurten, A.; St. Clair, J. M.; Seinfeld, J. H.; Wennberg, P. O. Unexpected Epoxide Formation in the Gas-Phase Photooxidation of Isoprene. *Science (80-.).* **2009**, *325* (5941), 730–733. https://doi.org/10.1126/science.1172910.

(36) Schwantes, R. H.; Teng, A. P.; Nguyen, T. B.; Coggon, M. M.; Crounse, J. D.; St. Clair, J. M.; Zhang, X.; Schilling, K. A.; Seinfeld, J. H.; Wennberg, P. O. Isoprene NO3 Oxidation Products from the RO2 + HO2 Pathway. *J. Phys. Chem. A* **2015**, *119* (40), 10158–10171. https://doi.org/10.1021/acs.jpca.5b06355.

(37) Nestorowicz, K.; Jaoui, M.; Rudzinski, K. J.; Lewandowski, M.; Kleindienst, T. E.; Spólnik, G.; Danikiewicz, W.; Szmigielski, R. Chemical Composition of Isoprene SOA under Acidic and Non-Acidic Conditions: Effect of Relative

Humidity. *Atmos. Chem. Phys.* **2018**, *18* (24), 18101–18121. https://doi.org/10.5194/acp-18-18101-2018.

(38)   Kwan, A. J.; Chan, A. W. H.; Ng, N. L.; Kjaergaard, H. G.; Seinfeld, J. H.; Wennberg, P. O. Peroxy Radical Chemistry and OH Radical Production during the NO $_3$ -Initiated Oxidation of Isoprene. *Atmos. Chem. Phys.* **2012**, *12* (16), 7499–7515. https://doi.org/10.5194/acp-12-7499-2012.

(39)   Surratt, J. D.; Gómez-González, Y.; Chan, A. W. H.; Vermeylen, R.; Shahgholi, M.; Kleindienst, T. E.; Edney, E. O.; Offenberg, J. H.; Lewandowski, M.; Jaoui, M.; et al. Organosulfate Formation in Biogenic Secondary Organic Aerosol. *J. Phys. Chem. A* **2008**, *112* (36), 8345–8378. https://doi.org/10.1021/jp802310p.

(40)   Schwantes, R. H.; Charan, S. M.; Bates, K. H.; Huang, Y.; Nguyen, T. B.; Mai, H.; Kong, W.; Flagan, R. C.; Seinfeld, J. H. Low-Volatility Compounds Contribute Significantly to Isoprene Secondary Organic Aerosol (SOA) under High-NO&Lt;Sub&Gt;&Lt;I&Gt;X&Lt;/I&Gt;&Lt;/Sub&Gt; Conditions. *Atmos. Chem. Phys.* **2019**, *19* (11), 7255–7278. https://doi.org/10.5194/acp-19-7255-2019.

(41)   Kwan, A. J.; Chan, A. W. H.; Ng, N. L.; Kjaergaard, H. G.; Seinfeld, J. H.; Wennberg, P. O. Peroxy Radical Chemistry and OH Radical Production during the NO&Lt;Sub&Gt;3&Lt;/Sub&Gt;-Initiated Oxidation of Isoprene. *Atmos. Chem. Phys.* **2012**, *12* (16), 7499–7515. https://doi.org/10.5194/acp-12-7499-2012.

(42)   Wennberg, P. O.; Bates, K. H.; Crounse, J. D.; Dodson, L. G.; McVay, R. C.; Mertens, L. A.; Nguyen, T. B.; Praske, E.; Schwantes, R. H.; Smarte, M. D.; et al. Gas-Phase Reactions of Isoprene and Its Major Oxidation Products. *Chem. Rev.* **2018**, *118* (7), 3337–3390. https://doi.org/10.1021/acs.chemrev.7b00439.

(43)   Cole-Filipiak, N. C.; O'Connor, A. E.; Elrod, M. J. Kinetics of the Hydrolysis of Atmospherically Relevant Isoprene-Derived Hydroxy Epoxides. *Environ. Sci. Technol.* **2010**, *44* (17), 6718–6723. https://doi.org/10.1021/es1019228.

(44)   Darer, A. I.; Cole-Filipiak, N. C.; O'Connor, A. E.; Elrod, M. J. Formation and Stability of Atmospherically Relevant Isoprene-Derived Organosulfates and Organonitrates. *Environ. Sci. Technol.* **2011**, *45* (5), 1895–1902. https://doi.org/10.1021/es103797z.

(45)   Salo, K.; Hallquist, M.; Jonsson, Å. M.; Saathoff, H.; Naumann, K.-H.; Spindler, C.; Tillmann, R.; Fuchs, H.; Bohn, B.; Rubach, F.; et al. Volatility of Secondary Organic Aerosol during OH Radical Induced Ageing. *Atmos. Chem. Phys.* **2011**, *11* (21), 11055–11067. https://doi.org/10.5194/acp-11-11055-2011.

(46)   Müller, L.; Reinnig, M.-C.; Naumann, K. H.; Saathoff, H.; Mentel, T. F.; Donahue, N. M.; Hoffmann, T. Formation of 3-Methyl-1,2,3-Butanetricarboxylic Acid via Gas Phase Oxidation of Pinonic Acid – a Mass Spectrometric Study of SOA Aging. *Atmos. Chem. Phys.* **2012**, *12* (3), 1483–1496. https://doi.org/10.5194/acp-12-1483-2012.